THE JOURNAL OF BIOLOGICAL CHEMISTRY VOL. 281, NO. 7, pp. 4274–4284, February 17, 2006

Purinergic Receptors Mediate Two Distinct Glutamate Release Pathways in Hippocampal Astrocytes*

Received for publication, September 30, 2005, and in revised form, November 10, 2005 Published, JBC Papers in Press, December 6, 2005, DOI 10.1074/jbc.M510679200

Tommaso Fellin, Tullio Pozzan, and Giorgio Carmignoto[1]

From the Consiglio Nazionale delle Ricerche Istituto di Neuroscienze and Dipartimento di Scienze Biomediche Sperimentali, Università di Padova, viale G. Colombo 3, 35121 Padova, Italy

The purinergic $P2X_7$ receptor ($P2X_7R$) can mediate glutamate release from cultured astrocytes. Using patch clamp recordings, we investigated whether $P2X_7Rs$ have the same action in hippocampal astrocytes *in situ*. We found that 2- and 3-*O*-(4-benzoylbenzoyl)ATP (BzATP), a potent, although unselective $P2X_7R$ agonist, triggers two different glutamate-mediated responses in CA1 pyramidal neurons; they are transient inward currents, which have the kinetic and pharmacological properties of previously described slow inward currents (SICs) due to Ca^{2+}-dependent glutamate release from astrocytes, and a sustained tonic current. Although SICs were unaffected by $P2X_7Rs$ antagonists, the tonic current was inhibited, was amplified in low extracellular Ca^{2+}, and was insensitive to glutamate transporter and hemichannel inhibitors. BzATP triggered in astrocytes a large depolarization that was inhibited by $P2X_7R$ antagonists and amplified in low Ca^{2+}. In low Ca^{2+} BzATP also induced lucifer yellow uptake into a subpopulation of astrocytes and CA3 neurons. Our results demonstrate that purinergic receptors other than the $P2X_7R$ mediate glutamate release that evokes SICs, whereas activation of a receptor that has features similar to the $P2X_7R$, mediates a sustained glutamate efflux that generates a tonic current in CA1 neurons. This sustained glutamate efflux, which is potentiated under non-physiological conditions, may have important pathological actions in the brain.

Glutamate is the principal mediator of excitatory neurotransmission in the central nervous system as well as a recognized excitotoxic agent that can lead neurons and astrocytes to death when present at excessive extracellular concentrations (1, 2). The ability to release this transmitter (3–5) hints at direct participation of astrocytes in glutamatergic neuronal transmission as well as in the excitotoxic action of glutamate. Although this latter issue remains to be proved, increasing evidence indicates that astrocyte-derived glutamate has complex actions on neurons exerting a modulatory role on synaptic transmission. For example, in the retina the release of glutamate from astrocytes modulates ganglion cell spike activity driven by light stimulation, most likely through a presynaptic action (6). In the hippocampus, it modulates excitability of interneurons and potentiates inhibitory transmission (7, 8); it acts also on excitatory axon terminals of the CA1 region to increase the probability of spontaneous glutamate release (9). At the same time, astrocytic glutamate exerts a direct action on hippocampal pyramidal neurons by activating extrasynaptic NMDARs[2] and triggering episodic, inward currents characterized by slow kinetics (SICs) (10, 11). Interestingly, this NMDAR response can occur synchronously in multiple CA1 neurons, raising the possibility that it may serve to promote synchrony of neuronal activity (10, 11).

As to the mechanism of glutamate release, it is known that $[Ca^{2+}]_i$ elevations in astrocytes can rapidly trigger the fusion with the plasma membrane of glutamate-containing vesicles (12, 13). Although this exocytosis-mediated pathway is most likely involved in astrocyte-to-neuron signaling under physiological conditions, other mechanisms may contribute to this process under both physiological and pathological conditions (14, 15). Recently, a glutamate release mechanism that involves the $P2X_7R$ has been proposed (16). This receptor has an established role in cellular toxicity and inflammatory processes (17, 18). Upon sustained activation with ATP, it can form a pore permeable to molecules of relatively large size (<900 Da), thus allowing molecules, such as glutamate, to efflux from, or enter into the cytoplasm according to their concentration gradient. In support of the role of the $P2X_7R$, the release of glutamate from murine-cultured astrocytes triggered by purinergic receptor agonists has been described (16) to be (i) larger upon stimulation with BzATP than with ATP (the latter being a weak $P2X_7R$ agonist), (ii) greatly potentiated in divalent ion-free medium, *i.e.* a condition that favors $P2X_7R$ openings, and (iii) blocked by $P2X_7R$ antagonists.

Although these results from cultured astrocytes clearly indicate that under selected experimental conditions the $P2X_7R$ allows the efflux of glutamate into the extracellular space, no such evidence exists for astrocytes *in situ*. On the other hand, at physiological concentrations of extracellular Ca^{2+}, ATP is known to trigger a significant release of glutamate from astrocytes (19, 20), which in this case depends on a classic Ca^{2+}-dependent pathway. Indeed, by activating both ionotropic, Ca^{2+}-permeable P2XRs, including the $P2X_7R$ and/or metabotropic P2YRs, ATP can evoke an intracellular Ca^{2+} increase that in turn mediates glutamate release.

The aim of this study was to gain insights into the role of the purinergic receptor $P2X_7$ in the generation of glutamate release from *in situ* astrocytes. Results obtained in patch clamp recordings from neurons and astrocytes of acute hippocampal slices allow us to conclude that $P2X_7R$ activation is not involved in the episodic glutamate release that triggers SICs. In contrast, a $P2X_7$-like receptor, possibly expressed in astrocytes and neurons, contributes significantly to increasing the extracellular concentration of glutamate, in particular when extracellular Ca^{2+} decreases to very low levels.

* This work was supported by grants from the Armenise-Harvard University Foundation, Italian University and Health Ministries (FIRB) Grant RBNE01RHZM_003 (to G. C), the Italian Association for Cancer Research (AIRC), and European Community Grant QLG3-CT-2000-00934) (to T. P.). The costs of publication of this article were defrayed in part by the payment of page charges. This article must therefore be hereby marked "*advertisement*" in accordance with 18 U.S.C. Section 1734 solely to indicate this fact.

[1] To whom correspondence should be addressed. Tel.: 39-049-8276075; Fax: 39-049-8276049; E-mail: gcarmi@bio.unipd.it.

[2] The abbreviations used are: NMDAR, *N*-methyl-D-aspartate (NMDA) receptor; $P2X_7R$, purinergic $P2X_7$ receptor; $[Ca^{2+}]_i$, intracellular Ca^{2+} concentration; BzATP, 2- and 3-*O*-(4-benzoylbenzoyl)ATP; SIC, slow inward current; TTX, tetrodotoxin; LY, lucifer yellow; D-AP5, D-(−)-2-amino-5-phosphonopentanoic acid; NBQX, 2,3-dioxo-6-nitro-1,2,3,4-tetrahydrobenzo[*f*]quinoxaline-7-sulfonamide; TBOA, DL-threo-β-benzyloxyaspartate; α,β-mATP, α,β-methylene ATP; BBG, Brilliant Blue G; OxATP, adenosine 5-triphosphate-2,3-dialdehyde; AMPA, α-amino-3-hydroxy-5-methyl-4-isoxazolepropionic acid.

MATERIALS AND METHODS

Slice Preparation—Transverse hippocampal slices (350–400 μm) were prepared as previously described (4, 21) from Wistar rats at postnatal days 10–23. After cutting, slices were incubated at 37 °C for a recovery period of at least 1 h. Slice cutting and incubation was performed with the following physiological saline solution: 120 mM NaCl, 3.2 mM KCl, 1 mM KH_2PO_4, 26 mM $NaHCO_3$, 2 mM $MgCl_2$, 1 mM $CaCl_2$, 2.8 mM glucose, 2 mM sodium pyruvate, and 0.6 mM ascorbic acid at pH 7.4 with 95% O_2, 5% CO_2. Slice incubation with 300 μM OxATP for 2–3 h and with 2–4 μM BBG for either 30 min or 1 h was carried out at 37 °C. When incubated with BBG for 30 min, slices were preincubated for 30 min in saline at 37 °C. As appropriate controls in OxATP and BBG experiments, we used slices maintained at 37 °C for either 1 or 2–3 h, respectively, and the recordings from these slices was performed the same days of the recordings from BBG- or OxATP-incubated slices. Recordings were also performed from additional neurons from control slices on days different from the days in which BBG and OxATP experiments were performed. Because the mean values of SIC frequency and tonic current amplitude from the different control experiments were similar, data from these experiments were pooled together.

Patch Clamp Recordings and Data Analysis—Most of the experimental procedures are similar to that described previously (11). In brief, during recordings slices were perfused with the following saline solution: 120 mM NaCl, 3.2 mM KCl, 1 mM KH_2PO_4, 26 mM $NaHCO_3$, 2 mM $CaCl_2$, 2.8 mM glucose, and 1 μM glycine at pH 7.4 with 95% O_2, 5% CO_2. Low Ca^{2+} solution was obtained by replacing $CaCl_2$ with EGTA (0.25 mM). Intracellular pipette solution was 145 mM potassium gluconate, 2 mM $MgCl_2$, 5 mM EGTA, 2 mM Na_2ATP, 0.2 mM NaGTP, and 10 mM HEPES to pH 7.2 with KOH. Slices were viewed with an upright Zeiss Axioscope microscope (Carl Zeiss Spa, Milan, IT) equipped with differential interference Nomarski optics, a CCD camera (COHU Inc., San Diego, CA), and a mercury light source for fluorescence excitation. Data were amplified and filtered at 1 KHz with one or two Axopatch-200B amplifiers and sampled at 5 KHz with a Digidata 1200 interface (Axon instruments, Union City, CA). The liquid junction potential at the pipette tip was −15 mV. This value should be added to all voltages to obtain the correct value of the membrane potential in whole-cell configuration. Series resistance ($6 < R_S < 15$ megaohms) was monitored throughout each experiment, and no compensation of R_S was applied. All experiments were performed at either room temperature or 35 °C and in the presence of TTX. Astrocytes were identified on the basis of both morphological and electrophysiological criteria. Astrocytes typically have small and round cell soma (diameter 6–10 μm), lack optically apparent large processes, do not fire action potentials upon application of depolarizing current pulses, and have a low input resistance (mean: 15.5 ± 1.9 megaohms, $n = 24$) and highly negative resting potentials (mean, −77.3 ± 0.7 mV, $n = 24$). All the astrocytes considered in this study exhibited a linear I-V relationship, typical of passive astrocytes (22). Neurons were voltage-clamped at −60 mV and astrocytes at −75 mV. Clampfit 8.2 (Axon instrument) and Origin 6.0 (Microcal Software, Northampton, MA) software were used for data analysis and fitting.

Transient inward currents with rise time slower than 10 ms and amplitude greater than −20 pA were classified as SICs. SIC frequency, amplitude, and kinetics were measured as described previously (11). In pair recording experiments, the time interval between two SICs was measured as the time interval between the onset of the current in cell 1 and the onset of the current in cell 2. Background noise amplitude was calculated as the peak-to-peak amplitude. Student's *t* test was performed to determine statistical significance. Data are expressed as mean ± S.E.

Ca^{2+} Imaging and Dye Uptake—Slice incubation with 10 μM Rhod-2 AM (Molecular Probes, Eugene, OR) and 0.02% pluronic for 50 min at 37 °C under mild stirring resulted in the selective loading of the Ca^{2+} indicator into astrocytes (23). A confocal laser scanning microscope (TCS SP2 RS, Leica, Mannheim, Germany) was used for monitoring the BzATP-induced $[Ca^{2+}]_i$ change in these cells. Slices were continuously perfused at room temperature with the same extracellular solution as used in electrophysiological recording with 0.2 mM sulfinpyrazone. The sampling rate was 2–4 s, and 8 images were averaged for each frame. Rhod-2 fluorescence was excited at 543 nm, and emitted light above 550 nm was collected. The fluorescent signal at a given time point was expressed as $\Delta F/F = (F_1 - F_0)/F_0$, where F_0 and F_1 are the values of the fluorescence in astrocytes at rest and at the given time point, respectively. No background subtraction was applied.

Dye uptake experiments were carried out incubating slices for 5–15 min with 1 μM TTX, 0.5 mg/ml lucifer yellow (LY) with or without 100 μM BzATP in the same solution used in patch clamp recording experiments under mild stirring and continuous bubbling with 95% O_2, 5% CO_2 to maintain pH 7.4. Incubation was terminated by washing in physiological saline, and fluorescence imaging was performed within 30 min. Fluorescence images were obtained with the same Leica confocal microscope using 458-nm excitation for LY. Cells were visually identified from the differential interference contrast image, and fluorescence intensity was measured from individual cells as the average intensity of fluorescence in a region of interest corresponding to the cell soma. No background subtraction was applied. In the 8-bit scale, a value of fluorescence intensity corresponding to 50 arbitrary units (3-fold the average background noise value: 17.7 ± 0.8 arbitrary units, $n = 475$) was chosen as the threshold for classifying positive cells. Background noise was not different in control slices and in slices incubated with BzATP or BzATP and low Ca^{2+}. Because of possible damage caused by slice cutting procedures, cells located close to the surface may unspecifically take up the dye. Therefore, cells positively loaded with the dye were considered only when they were located below the first 10–15 μM from the surface.

Drugs—D-AP5, NBQX, 2-methyl-6-(phenylethynyl)pyridine hydrochloride, LY367385 ((*S*)-(+)- α-amino-4-carboxy-2-methyl-benzeneacetic acid), TBOA, and TTX were purchased from Tocris Cookson (Buckhurst Hill, UK), and BzATP, α,β-mATP, BBG, OxATP, LY, and carbenoxolone were from Sigma. All chemicals were dissolved in water or Me_2SO and then diluted in the recording physiological solution just before use.

RESULTS

Purinergic Receptor Stimulation Evokes Transient and Sustained Activation of Neuronal NMDA Receptors—In hippocampal slices in the absence of extracellular Mg^{2+} and in the presence of 1 μM TTX, BzATP (100 μM), a potent although unselective agonist of $P2X_7R$ (24, 25), evokes a complex response in 20 of 39 (51%) CA1 pyramidal neurons consisting of episodic, transient inward currents and a slowly developing tonic current (Fig. 1, *A* and A_1). Transient inward currents had a low frequency and could occur also spontaneously (Fig. 1*B*). The tonic current initiated 1–2 min after the onset of the BzATP application had a mean amplitude of −80 ± 23 pA and a mean time to peak of 98 ± 9 s, and it was always associated with a more than 2-fold increase in the background noise of the current trace ($n = 13$, Fig. 1*C*). Both transient currents and the tonic current were detected in 6 of the 20 (30%) responsive neurons (Fig. 1, *A* and A_1), whereas either the tonic current or transient currents were observed in 7 (35%) and 7 (35%) of the responsive neurons, respectively (Fig. 1, *D* and *E*).

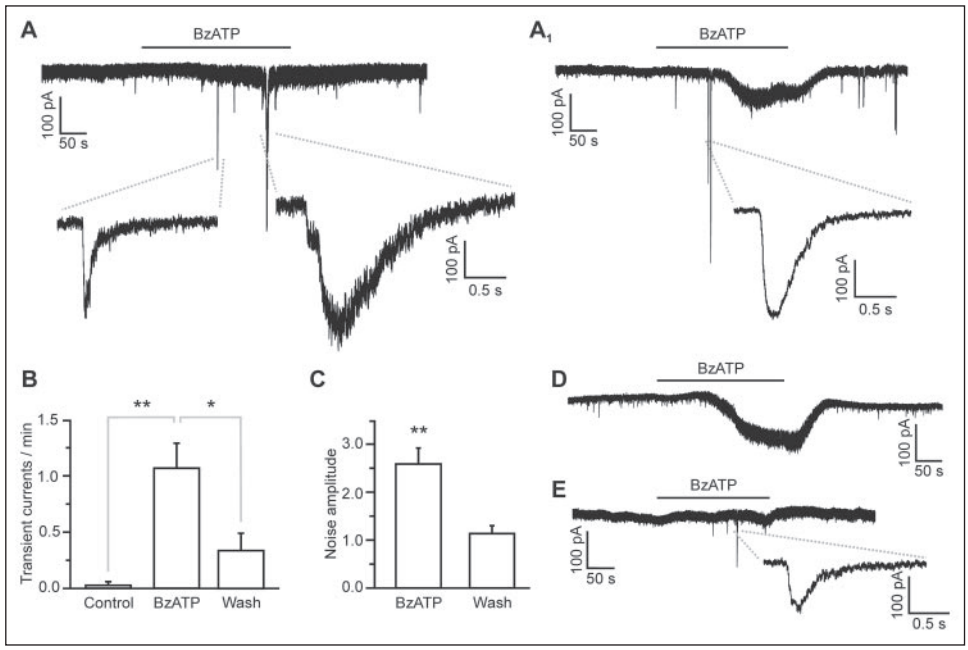

FIGURE 1. **Slice perfusion with BzATP triggers complex responses in CA1 pyramidal neuron.** *A–A$_1$*, *top*, representative whole-cell patch clamp recordings from two neurons showing the transient inward currents and the tonic current triggered by BzATP application (*thick line*). *Bottom*, transient inward currents at an expanded timescale. *B*, average number of transient currents/min before, during, and after BzATP application in 10 of the 13 responsive neurons. Three neurons had a significantly higher frequency of spontaneous transient currents (7.3 ± 2.0 SIC/min; $p < 0.001$) and were not included in the mean. In these three neurons the frequency of the transient currents in the presence of BzATP was 9.6 ± 3.4 transient currents/min. *B* and *C*, *, $p < 0.05$; **, $p < 0.01$. *C*, average value of the background noise during BzATP application and after its washout in the 13 neurons that responded with a tonic current to BzATP application. Data are normalized to the noise amplitude before BzATP application. *D–E*, patch clamp recording from a pyramidal neuron displaying the tonic current but not transient currents (*D*) or transient currents but not the tonic current (*E*) in response to BzATP.

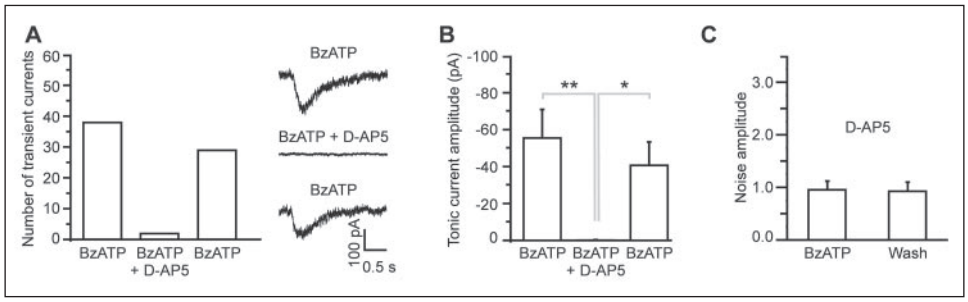

FIGURE 2. **BzATP-induced neuronal responses are due to activation of NMDA receptors.** *A*, total number of transient currents evoked by a 3-min application of BzATP in control conditions in the presence of D-AP5 and after D-AP5 washout ($n = 4$ neurons). *Inset*, current recordings from a representative neuron under the different experimental conditions. *B*, average amplitude values of the BzATP-evoked tonic current in control conditions in the presence of D-AP5 and after D-AP5 washout ($n = 5$ neurons). *, $p < 0.05$; **, $p < 0.01$. *C*, openings of the NMDAR mediate the increase in background noise. The same five neurons as in *B* are shown. Average values of background noise in the continuous presence of D-AP5 during BzATP application and after its washout. Data are normalized to the noise amplitude in the presence of D-AP5 before BzATP application.

Both the transient currents (Fig. 2*A*) and the tonic current associated with noise increase (Fig. 2, *B* and *C*) evoked by BzATP were reversibly blocked by the NMDAR antagonist D-AP5 (50–100 μM) and can, thus, be attributed to the activation of NMDARs. These results clearly indicate that slice perfusion with BzATP triggers the release of glutamate that evokes in CA1 pyramidal neurons both transient and sustained activation of the NMDARs.

BzATP-induced noise increase is not due to an increase in the spontaneous synaptic release of glutamate since in the presence of D-AP5 and TTX, the frequency and amplitude of AMPA-mediated miniature currents under basal conditions and upon BzATP stimulation were not significantly changed (12 ± 9 *versus* 15 ± 13 events/min, $n = 4$; −7.7 ± 0.2 pA, $n = 115$, *versus* −8.1 ± 0.3 pA, $n = 176$; $p > 0.2$).

Glutamate Release from Astrocytes Mediates the Transient Neuronal Response—Elevations in the $[Ca^{2+}]_i$ evoked in hippocampal CA1 astrocytes by various stimuli, including purinergic receptor agonists, have been recently shown to trigger a pulsatile release of glutamate from these cells (11). Glutamate released from activated astrocytes acts primarily on extrasynaptic NMDARs of CA1 pyramidal neurons to trigger episodic inward currents with characteristic slow kinetics that we have called SICs (11). The transient, slow events evoked by BzATP in CA1 pyramidal neurons described above are mediated exclusively by NMDARs and are insensitive to 1 μM TTX. Therefore, they have the same pharmacological profile of SICs (11) as well as of the slow currents described by Angulo *et al.* (10). As shown in Fig. 3*A*, the mean rise time of BzATP-induced transient currents is 70.1 ± 7.9 ms ($n = 54$), one order of magnitude larger than that of excitatory postsynaptic currents evoked in the same neurons by Schaffer collateral stimulation (rise time, 6.7 ± 0.5 ms, $n = 22$). The mean decay time was 376.5 ± 24.4 ms (Fig. 3*B*; $n = 54$), which is slower than that of the excitatory postsynaptic currents from the same neurons ($\tau_1 = 17.9 \pm 6.7$ ms, $\tau_2 = 195.5 \pm 14.7$ ms, $n = 22$). The amplitude of these events can reach several hundred pA, with a mean of −115.9 ± 15.6 pA (Fig. 3*C*; $n = 54$). These features are also typical of SICs, providing further evidence for the classification of BzATP-evoked transient currents as SICs.

An additional feature of SICs is that they occur with a high degree of synchrony in different pyramidal neurons (10, 11). We investigated this issue by using patch clamp pair recordings from two pyramidal neurons. In two of the four pairs that displayed the transient currents upon BzATP stimulation, synchronous events were observed (Fig. 3*D*). The inter-event time interval histogram (Fig. 3*E*) shows that, similar to SICs, 42% of these events (40 of 96) are synchronized in a time window of 200 ms. Taken together, these data suggest that the BzATP-induced transient currents have the same pharmacological and biophysical properties of SICs, *i.e.* the

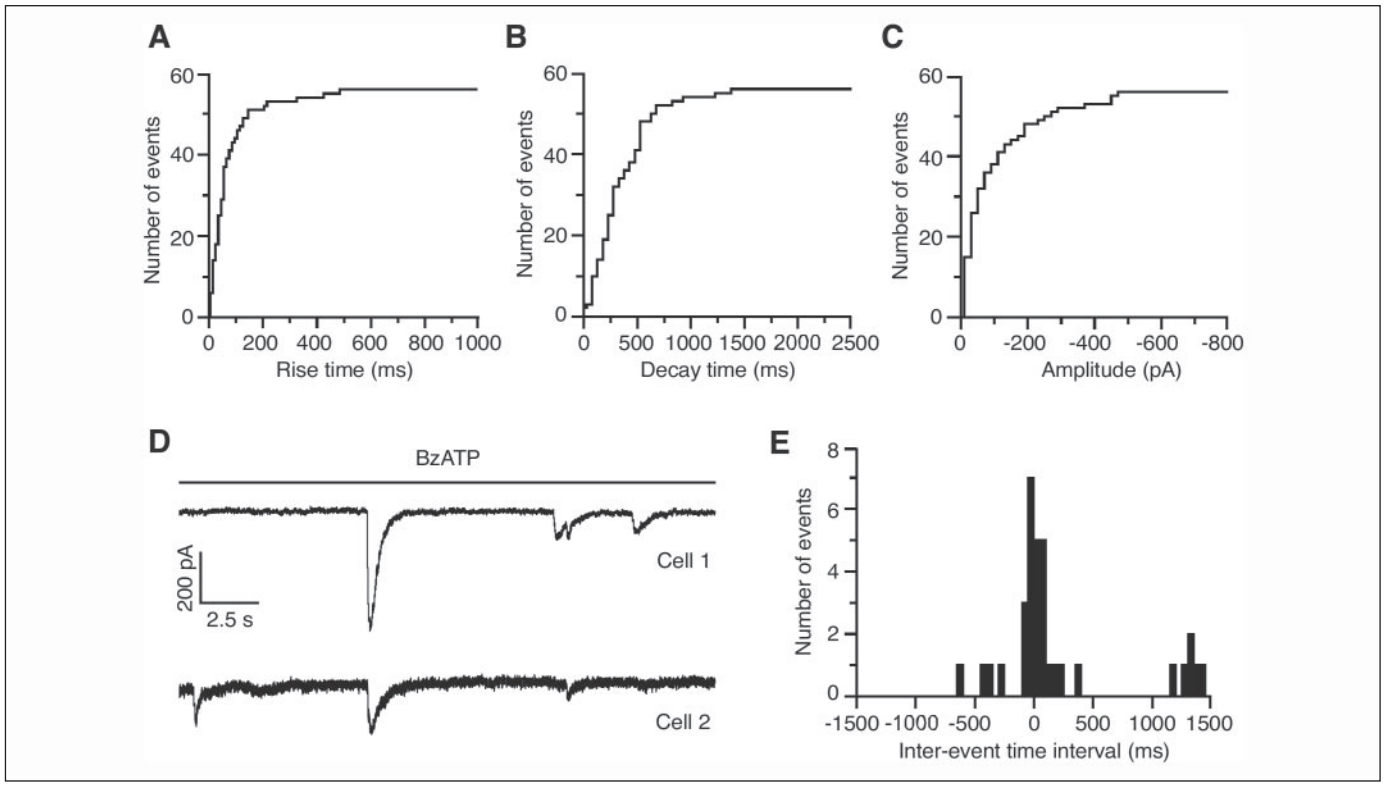

FIGURE 3. **The transient neuronal responses are SICs.** *A–C*, cumulative distribution of rise time (*A*, bin 10 ms), decay time (*B*, bin 50 ms), and amplitude (*C*, bin 20 pA) of BzATP-evoked transient currents from 13 responsive neurons. *D*, synchronized BzATP-evoked transient currents from two pyramidal neurons. *E*, inter-event time interval histogram of transient currents occurring in the two neurons from two different pairs. A total number of 40 time intervals were counted in a time window of ± 2 s. Note that 40 transient currents, *i.e.* 20 of these time intervals, are restricted within a time window of 200 ms. Bin, 50 ms.

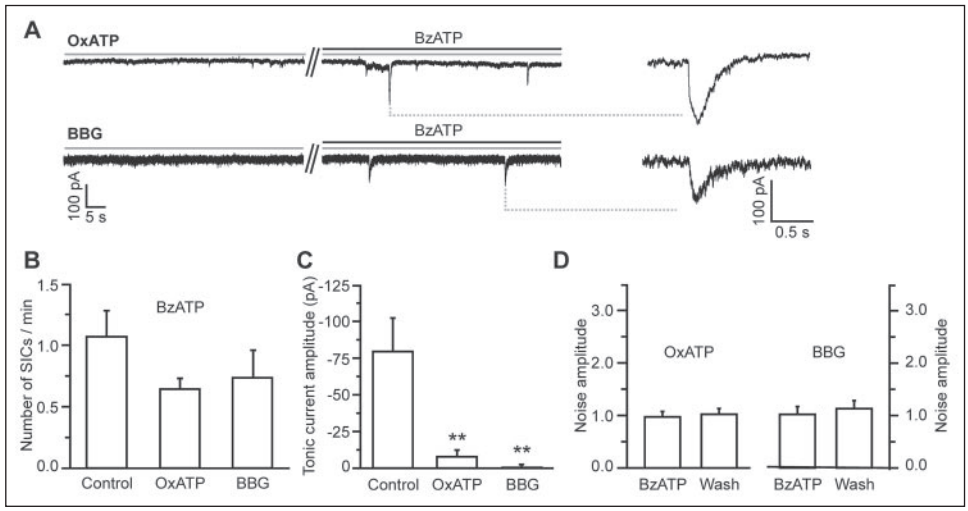

FIGURE 4. **Slice incubation with OxATP or BBG abolishes the BzATP-evoked tonic current but does not affect SICs.** *A*, example of BzATP-evoked SICs in the presence of OxATP (300 μM, *top*) and BBG (2 μM, *bottom*), respectively. *B*, average frequency of BzATP-evoked SICs in control condition ($n = 13$) and in slices incubated in OxATP ($n = 8$) or BBG ($n = 7$). *C*, average amplitude values of the BzATP-evoked tonic current in control slices ($n = 13$) and in slices incubated in OxATP ($n = 15$) or BBG ($n = 13$). *, $p < 0.05$; **, $p < 0.01$. *D*, mean amplitude value of the background noise during BzATP application and after its washout in slices incubated with OxATP (*left*, $n = 15$) or BBG (*right*, $n = 13$). Data are normalized to the noise amplitude before BzATP application.

NMDAR-mediated, slow inward currents that are triggered in CA1 pyramidal neurons by glutamate released from activated astrocytes.

SIC and Tonic Current Generation Is Dependent on the Activation of Different Purinergic Receptors—Given that BzATP is known to be a strong agonist of the P2X$_7$R, we next investigated the possible involvement of this receptor in the generation of the BzATP-induced SICs and tonic current. To this aim, we used OxATP (300 μM) or BBG (2–4 μM), which efficiently block the P2X$_7$R (24, 26, 27), although they probably also affect other P2XRs. In the presence of OxATP or BBG, BzATP triggered SICs (Fig. 4*A*) in 7 of 18 (39%) and in 8 of 19 (42%) neurons, respectively. The percentage of responsive neurons, the frequency of the BzATP-induced SICs, and their amplitude and kinetics were not significantly different from controls (Fig. 4*B*; Table 1). Interestingly, under these conditions and in all the neurons tested, BzATP failed to trigger a tonic current (Fig. 4*C*) or an increase in background noise (Fig. 4*D*). These data demonstrate that, on the one hand, SICs generation is not mediated by P2X$_7$ receptors and, on the other, that the generation of the tonic current is dependent upon the activation of a purinergic receptor type that is blocked by OxATP and BBG.

Support for this hypothesis derives from the observation that other stimuli used to trigger SICs, such as (*S*)-3,5-dihydroxyphenylglycine, prostaglandin E$_2$, or photolysis of caged-Ca^{2+}, did not evoke a tonic current associated with an increase in background noise (11). Interestingly, 100 μM α,β-mATP, a purinergic agonist different from BzATP

TABLE 1

Amplitude and kinetics of SICs are independent of P2X$_7$R activation

Mean ± S.E., and range for the amplitude and rise and decay time of SICs evoked by BzATP or α,β-mATP under the various experimental conditions are shown.

	Amplitude	Rise time	Decay time	*n*
	pA	*ms*	*ms*	
BzATP	−115.9 ± 15.6 (−23.0 to −496.2)	70.1 ± 7.9 (10.2 to 334.6)	376.5 ± 24.4 (42.9 to 1412.5)	54
BzATP + BBG	−94.9 ± 9.8[a] (−20.1 to −260.0)	53.3 ± 8.0[a] (11.0 to 298.6)	347.5 ± 48.4[b] (63.1 to 1546.4)	47
BzATP + OxATP	−98.5 ± 15.2[a] (−23.0 to −342.9)	62.4 ± 8.4[b] (16.8 to 256.0)	318.6 ± 50.3[a] (74.9 to 1398.8)	34
α,β-mATP	−109.6 ± 31.1[b] (−23.5 to −636.2)	70.4 ± 11.9[b] (13.8 to 184.2)	449.3 ± 53.4[a] (184.3 to 933.6)	19
BzATP + 0 Ca^{2+}	−216.7 ± 57.8[c] (−21.0 to −695.2)	86.1 ± 18.4[a] (13.1 to 206.4)	490.4 ± 108.8[a] (61.9 to 1327.5)	13

[a] $p > 0.1$.
[b] $p > 0.5$.
[c] $p < 0.05$.

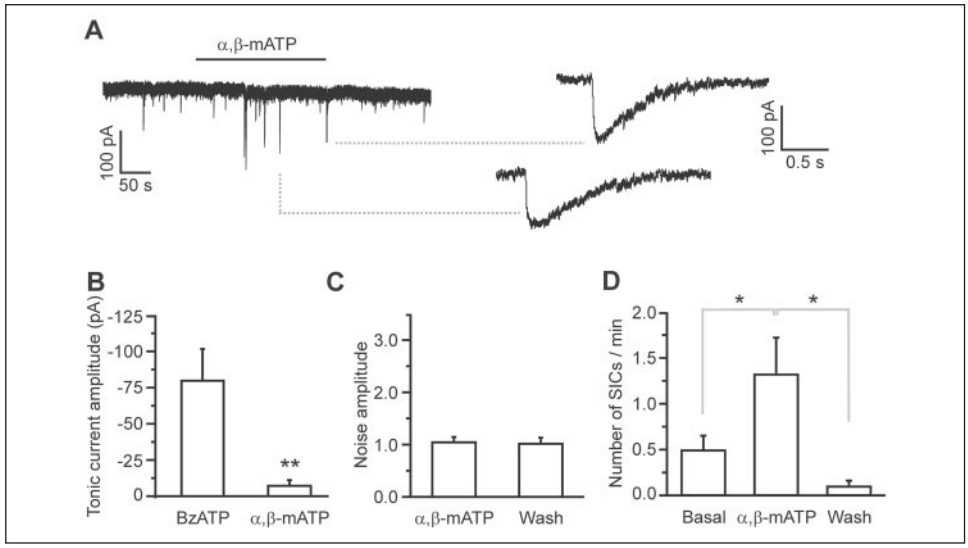

FIGURE 5. **Stimulation with α,β-mATP triggers SICs but not the tonic current.** *A*, representative example of SICs evoked by slices perfusion with α,β-mATP (100 μM). *B*, average amplitude values of the tonic current evoked by BzATP (100 μM, $n = 13$) and α,β-mATP (100 μM, $n = 13$). *C*, average noise amplitude during α,β-mATP application and after its washout ($n = 13$). *D*, mean frequency of SICs under control conditions, during α,β-mATP application, and after its washout in six responsive neurons. *B* and *D*, *, $p < 0.05$; **, $p < 0.01$.

(24, 25), also failed to trigger either a tonic current (Fig. 5, *A* and *B*; $n = 13$) or an increase in background noise (Fig. 5*C*). Conversely, α,β-mATP triggered SICs in 6 of 13 pyramidal neurons (46%) with frequency, amplitude, and kinetics similar to those of SICs evoked by BzATP (Fig. 5*D*; Table 1).

We also investigated the hypothesis that the action of Bz-ATP on neurons is mediated by adenosine receptors that can be activated by Bz-adenosine, a product of Bz-ATP degradation by ectonucleotidase enzymes. Results obtained show that application of 100 μM adenosine always failed to trigger a tonic current in CA1 neurons ($n = 13$, data not shown). As previously reported (28), we rather observed an outward current of a mean amplitude of 41.9 ± 4.5 pA.

To gain further insights into the possible involvement of the P2X$_7$R in the generation of the tonic current, we applied BzATP in the presence of low extracellular Ca^{2+}, a condition that results in a large increase in the P2X$_7$R conductance (29). To reduce the concentration of Ca^{2+} in the extracellular space, we perfused slices with saline containing 0.25 mM EGTA and no added Ca^{2+}. Noteworthy is that 20 min after the onset of slice perfusion with this saline, a depolarizing stimulus (60 mM K^+) still elicited $[Ca^{2+}]_i$ elevations in neurons (data not shown). Thus, we confirm previous observations (30) that the reduction of extracellular Ca^{2+} in slices is a slow process, and after perfusion with a saline containing 0 mM Ca^{2+} and 0.25 mM EGTA, sufficient Ca^{2+} remains in the extracellular space to elicit $[Ca^{2+}]_i$ elevations through voltage-gated Ca^{2+} channels.

In 7 neurons in which BzATP triggered either a clear (Fig. 6*A*, *top*, $n = 3$) or a nearly undetectable tonic current (Fig. 6A_1, *top*, $n = 4$) when a second BzATP challenge was performed in low extracellular Ca^{2+}, the amplitude of the tonic current was drastically increased (Fig. 6, *A* and A_1, *bottom*, and *B*, *left*). The increase in background noise, which is always associated with the tonic current, was similarly enhanced (Fig. 6*B*, *right*). In contrast, the kinetic features of SICs evoked by BzATP in low Ca^{2+} are unchanged with respect to SICs evoked by BzATP in normal Ca^{2+} (Table 1). Because of the fact that BzATP in low Ca^{2+} triggered a large increase in the background noise of the trace, SICs of small amplitude were lost in the noise, and thus, only SICs of larger amplitude could be analyzed. As such, the mean amplitude of SICs evoked by BzATP in low Ca^{2+} results are higher than the mean amplitude of SICs evoked by BzATP in normal Ca^{2+}.

Slice perfusion for 3–4 min with low Ca^{2+} in the absence of BzATP failed to evoke either a significant tonic current or an increase in noise amplitude ($n = 21$; Fig. 6, A_2 and *B*). As we showed previously (11), slice perfusion with low Ca^{2+} induces Ca^{2+} oscillations in astrocytes and, thus, activates the Ca^{2+}-dependent release of glutamate in these cells that leads to the generation of SICs in CA1 pyramidal neurons. Several SICs can indeed be detected in neurons upon low Ca^{2+} stimulation (Fig. 6A_2). D-AP5 (50–100 μM) reversibly abolished the tonic current evoked by application of BzATP in low Ca^{2+}, demonstrating that it is entirely due to glutamate-mediated activation of NMDA receptors (Fig. 6*C*). In the presence of the P2X$_7$R

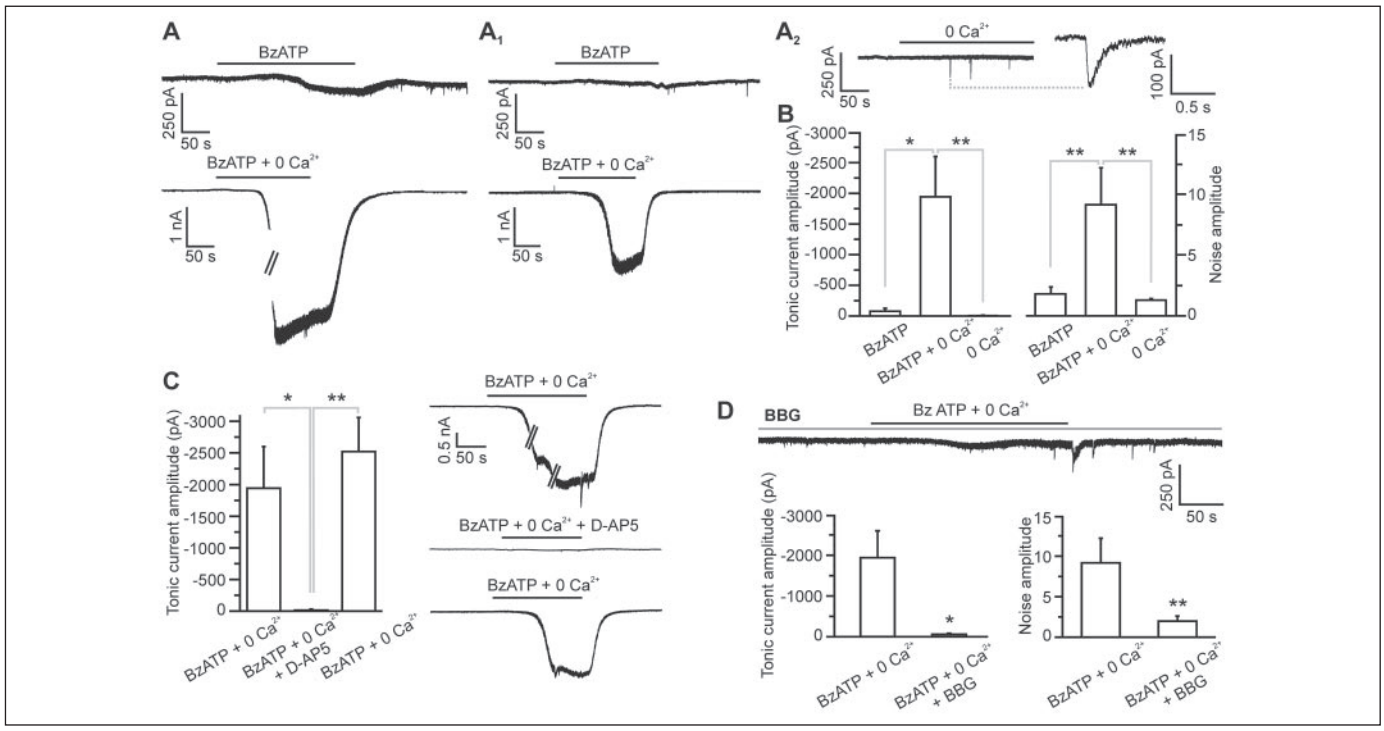

FIGURE 6. **The tonic current is greatly potentiated in the absence of extracellular Ca^{2+}.** *A* and A_1, two examples of BzATP-evoked tonic current in normal (*top*) and in low external Ca^{2+} (*bottom*). Because of the large amplitude of the tonic current, recordings had to be interrupted to change the gain (line break). A_2, low external Ca^{2+} triggers SICs but not the tonic current. *B*, average values of tonic current (*left*) and noise (*right*) amplitude in neurons upon BzATP ($n = 7$) and BzATP applied in 0 Ca^{2+} ($n = 7$) and 0 Ca^{2+} alone ($n = 21$). *C*, *left*, average amplitude of BzATP-evoked tonic current in the absence of external Ca^{2+} under control conditions ($n = 7$), during D-AP5 application ($n = 7$), and after D-AP5 washout ($n = 3$). *Right*, current recordings from a representative neuron under the different experimental conditions. *D*, *top*, example of tonic current evoked by BzATP in low external Ca^{2+}, in the presence of BBG (2 μM). *Bottom*, average amplitudes of the tonic current and noise triggered by BzATP in low external Ca^{2+} in the absence ($n = 7$) and in the presence of BBG ($n = 6$). *, $p < 0.05$; **, $p < 0.01$.

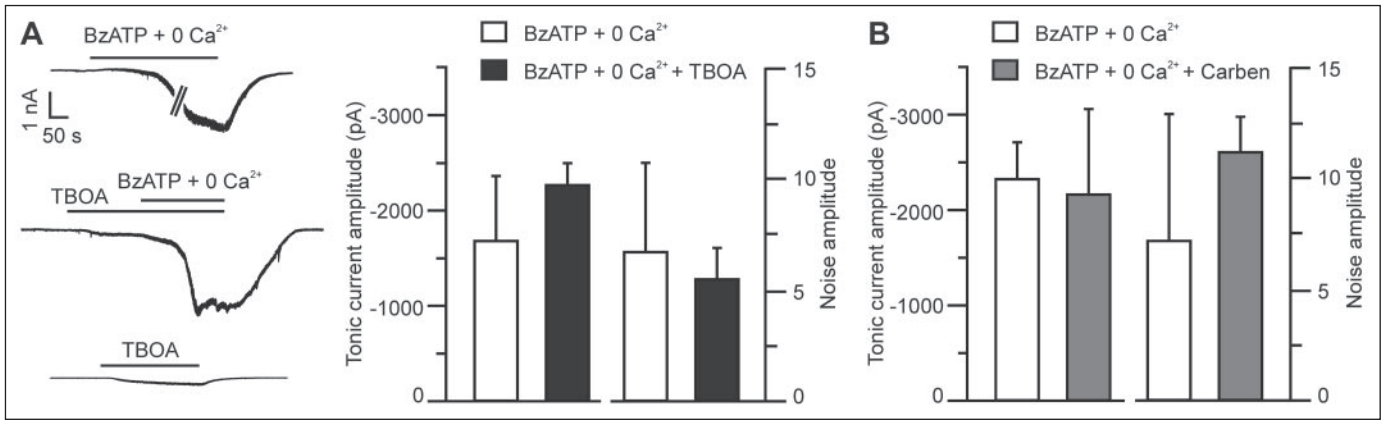

FIGURE 7. **The tonic current is independent of glutamate transporter operation and hemichannel openings.** *A*, the *bar graph* reports the average values of the tonic current (*left*) and noise (*right*) amplitude in neurons upon BzATP application in 0 Ca^{2+} in the absence ($n = 3$) and presence ($n = 3$) of TBOA (50 μM). Application of TBOA alone triggers a steady state, inward current of -186.0 ± 56.1 pA ($n = 3$). Tonic current amplitude in the presence of TBOA was calculated with respect to the TBOA-induced inward current. Controls were always recorded from slices of the same animal. In two experiments successive BzATP applications in 0 Ca^{2+} in the absence and presence of TBOA were performed on the same cell. Representative traces under the different experimental conditions are also shown. *B*, average values of the tonic current and noise amplitude in neurons upon BzATP application in 0 Ca^{2+} ($n = 3$) and in slices perfused with carbenoxolone (100 μM for 15–20 min, $n = 3$).

antagonist BBG (2 μM), BzATP application in low Ca^{2+} evoked a negligible tonic current and a small increase in background noise in 6 of 12 neurons (50%; Fig. 6*D*). Finally, application in low Ca^{2+} of the weak P2X$_7$R agonist α,β-mATP triggered in 4 of 6 neurons (67%) a tonic current of negligible amplitude compared with that triggered by BzATP under the same experimental conditions (not shown).

The reverse operation of glutamate transporters and opening of hemichannels are not involved in the BzATP-induced release of glutamate, which generates the tonic current (Fig. 7). Indeed, in the presence of the glutamate transporter inhibitor TBOA (31) or of the hemichannel antagonist carbenoxolone (100 μM, Fig. 7*B* (32, 33) both the amplitude of the tonic current and the increase in background noise triggered by 100 μM BzATP in low Ca^{2+} are unaffected ($p > 0.4$). The inhibition of glutamate uptake by TBOA results in an increase in the concentration of extracellular glutamate that, in the absence of BzATP stimulation, results in a steady state, inward current (Fig. 7*A*, *bottom trace*) with a mean amplitude of -186.0 ± 56.1 pA ($n = 3$). Taken together, these observations indicate that activation of the P2X$_7$R or of a P2X$_7$-like receptor in hippocampal slices results in the release of glutamate that mediates the tonic current.

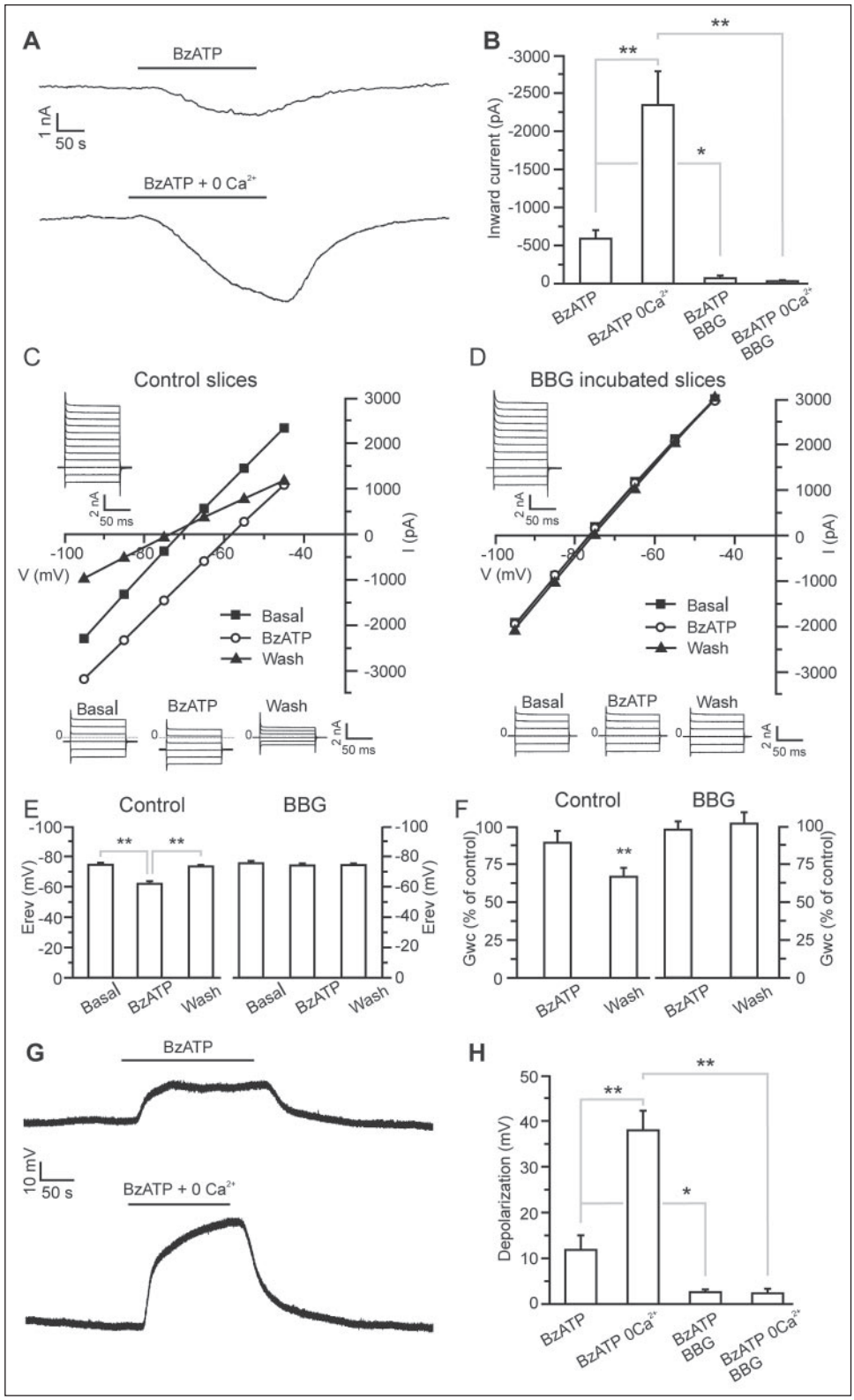

FIGURE 8. **Functional P2X$_7$-like receptors in stratum radiatum astrocytes.** *A*, voltage clamp recordings from a stratum radiatum astrocyte showing an inward current in response to BzATP in the presence (*top*) or absence (*bottom*) of external Ca^{2+}. *B*, average values of the astrocytic BzATP-induced inward current in the presence or absence of external Ca^{2+} in control slices ($n = 11$) and in slices preincubated with BBG ($n = 4$). *, $p < 0.05$; **, $p < 0.01$. *C*, representative experiment showing whole-cell I-V relationships under basal conditions, in the presence of BzATP (100 μM), and after BzATP washout from a passive astrocyte (see *top left inset*; voltage steps from −95 to +15 mV, holding potential −75 mV). In the presence of BzATP the voltage steps are applied when the BzATP-induced inward current reaches its maximum amplitude (between the second and the third minute of application). I-V relationships are obtained by applying to the membrane voltage steps from −95 to −45 mV (see the *bottom inset* for current traces; holding potential −75 mV). Voltage steps were restricted to this voltage range to limit inadequate clamping of high amplitude currents. A value of −15 mV should be added to all the voltages to correct for the liquid junction potential (see "Materials and Methods"). *D*, representative experiment showing whole-cell I-V relationships from an astrocytes of a slice incubated with 4 μM BBG. In the presence of BzATP, voltage steps are applied, as in control slices, between the second and third minute of BzATP application. *E*, average values of the reversal potential (E_{rev}) of the whole-cell I-V relationship in the different experimental conditions from control slices (*left*, $n = 5$) and from slices incubated with BBG (*right*, $n = 4$). *F*, average values of the whole-cell membrane conductance in the presence of BzATP and after its washout, in control slices (*left*, $n = 5$), and in slices incubated with BBG (*right*, $n = 4$). Conductance values are obtained from the slope of the linear fit of the whole-cell I-V relationships and are expressed as percentage of the value of the membrane conductance under resting conditions before BzATP application. *G*, current clamp recordings from a stratum radiatum astrocyte showing membrane depolarization in response to BzATP in the presence (*top*) or absence (*bottom*) of external Ca^{2+}. *H*, average values of the astrocytic depolarization in response to BzATP in the presence or absence of external Ca^{2+} in control slices ($n = 5$) and in slices preincubated with BBG ($n = 4$). *, $p < 0.05$; **, $p < 0.01$.

BzATP activates $[Ca^{2+}]_i$ elevations in astrocytes (34) that are known to trigger a Ca^{2+}-dependent release of glutamate from these cells (3, 5). The larger amplitude of the tonic current evoked by BzATP in low Ca^{2+} with respect to the amplitude of the tonic current evoked by BzATP in normal Ca^{2+} might, thus, be due to a higher number of astrocytes activated by BzATP in low Ca^{2+}. In contrast with this hypothesis, we found that the number of astrocytes displaying $[Ca^{2+}]_i$ elevations in response to BzATP (24 of 27; 89 ± 7%; $n = 3$) was similar to that observed after BzATP application in low Ca^{2+} (23 of 27; 84 ± 5%; $n = 3$, $p > 0.5$). Given that BzATP can also activate, besides various P2XRs, the P2Y$_1$R (25), BzATP may act also on this metabotropic receptor to trigger Ca^{2+} elevations in astrocytes. ATP-mediated Ca^{2+} responses in stratum radia-

tum astrocytes from mouse hippocampal slices have been indeed shown to be mediated by P2Y$_1$Rs (35).

BzATP Triggers in Astrocytes a Large Depolarization Mediated by a P2X$_7$-like Receptor—Murine astrocytes in culture have been shown to massively release glutamate through P2X$_7$R openings (16). To test whether functional P2X$_7$Rs are also expressed in *in situ* astrocytes and if they are involved in the generation of the tonic current, we performed patch clamp recordings from stratum radiatum astrocytes. In each of the cells tested ($n = 11$), BzATP (100 μM) evoked a slowly developing inward current (mean time to peak, 102 ± 12 s) that was greatly potentiated when BzATP was applied in low Ca^{2+} (Fig. 8, *A* and *B*). The current evoked by BzATP under both normal and low Ca^{2+} concentrations was almost abolished in the presence of BBG (Fig. 8*B*).

To directly test the hypothesis that BzATP opens in the astrocytic membrane a channel permeable to large molecules, such as a P2X$_7$-like receptor, we applied voltage steps to whole-cell recorded astrocytes. We found that in all astrocytes tested ($n = 5$), BzATP application reversibly shifted the reversal potential (E_{rev}) of the whole-cell I-V relationship toward more positive voltages with respect to basal conditions (Fig. 8, *C* and *E*). This shift was prevented in astrocytes from slices incubated with BBG (Fig. 8*D*, E; $n = 4$). Surprisingly, the overall membrane conductance was found to be unchanged upon BzATP application and to decrease drastically after BzATP washout (Fig. 8, *C* and *F*).

Given the low input resistance of the astrocytes and the huge current induced by BzATP, the voltage clamp measurements described above are affected by inadequate clamping of the astrocytic membrane to the imposed voltage. To address this concern we repeated the experiments in current clamp configuration. In all the astrocytes recorded ($n = 4$), BzATP evoked a slowly increasing depolarization of the astrocytic membrane (Fig. 8, *G* and *H*) which, as in the previous voltage-clamp experiments, is greatly potentiated when BzATP is applied in low external Ca^{2+} and almost completely blocked by BBG (Fig. 8*H*).

Activation of glutamate receptors by glutamate released from either astrocytes or neurons upon BzATP stimulation is not involved in the BzATP-induced inward current in astrocytes. Indeed, in the presence of 10 μM NBQX, 100 μM LY367385, and 50 μM 2-methyl-6-(phenylethynyl)pyridine hydrochloride, antagonists of the AMPA receptor, metabotropic glutamate receptor (mGluR) 1 and mGluR5, respectively, BzATP triggered in astrocytes an inward current of unchanged amplitude (−590.9 ± 104.3 pA, $n = 11$, and −552.8 ± 121.2 pA, $n = 4$, in the absence and in presence of the antagonists, respectively; $p > 0.5$). The BzATP-induced inward current was also unaffected in the presence of 50 μM D-AP5, antagonist of the NMDA receptor (mean amplitude: −561.7 ± 136.5 pA, $n = 3$, $p > 0.5$).

If the large inward current induced by BzATP in the astrocytic membrane is due to a large pore-forming purinergic receptor, it may allow the entrance of molecules of high molecular weight. When BzATP was applied in the virtual absence of external Ca^{2+}, a significant uptake of LY was detected in a subpopulation of astrocytes from the CA1 region (80 of 238, 29 ± 4%; $n = 8$) (Fig. 9, *C* (cells *2–5*) and *E*). Electrophysiological characterization of dye-loaded cells demonstrates that these cells display the passive membrane properties typical of astrocytes ($n = 3$, Fig. 9*E*).

In patch clamp experiments the BzATP-induced response triggered in low Ca^{2+} was observed in all astrocytes recorded, whereas BzATP in low Ca^{2+} induced loading of LY only in a subpopulation of these cells. We suggest that the higher sensitivity of patch clamp with respect to the dye uptake technique may account for this discrepancy. The dye uptake in astrocytes was inhibited in the presence of BBG (Fig. 9*E*). A BBG-sensitive dye uptake was also detected in a subpopulation of neurons from the CA3 region (71 of 168, 40 ± 5%; $n = 4$, Fig. 9, *D* and *F*).

After BzATP incubation, a few pyramidal neurons were also stained with LY in CA1 region. However, since the number of stained CA1 neurons from control slices was similar (Fig. 9*G*), the dye uptake in these neurons was independent of BzATP action and possibly reflects membrane damage after the slicing procedures.

Taken together, data from electrophysiological and dye uptake experiments support the view that a pore-forming receptor, such as the P2X$_7$R or a P2X$_7$-like receptor, possibly expressed in astrocytes as well as in neurons, can open and either directly or indirectly accounts for the release of glutamate that contributes to the generation of the tonic current in CA1 neurons, in particular under low Ca^{2+} conditions.

DISCUSSION

In the present study we found that activation of purinergic receptors in the hippocampus activates two separate pathways of glutamate release that trigger two distinct responses in CA1 pyramidal neurons. The first pathway depends on activation of purinergic receptors in astrocytes other the P2X$_7$R and mediates the episodic SIC in neurons. The second pathway depends on activation of a P2X$_7$-like receptor, expressed in either astrocytes and neurons, and mediates the sustained tonic current in neurons.

The episodic SIC was previously demonstrated to be due to Ca^{2+}-dependent glutamate release from astrocytes and to represent a form of glutamate-mediated astrocyte-to-neuron signaling that promotes synchronous activity of CA1 pyramidal neurons (10, 11). SICs evoked by BzATP, a powerful although unselective agonist of the P2X$_7$R, were shown here not to be affected by the P2X$_7$R antagonists BBG and OxATP (24, 26, 27). This finding rules out the possibility that BzATP acts on a P2X$_7$R to trigger the release of glutamate-mediating neuronal SICs. Beside the P2X$_7$R, BzATP is known to stimulate most of the other P2X receptors, although with different potencies (24, 25, 36). BzATP can also activate metabotropic P2YRs (25), including the P2Y$_1$R that in mouse stratum radiatum astrocytes mediates Ca^{2+} elevations triggered by ATP (35). Activation by BzATP of both Ca^{2+}-permeable P2XRs (37) and metabotropic P2YRs can, thus, lead to $[Ca^{2+}]_i$ elevations in the astrocytes and triggers the Ca^{2+}-dependent glutamate release pathway that mediates SICs. Our observations that α,β-mATP does not effectively activate either P2X$_7$Rs or P2YRs (24, 25) also evoke SIC support for the conclusion that activation of a P2XR other than the P2X$_7$R is sufficient to trigger the release of glutamate from astrocytes that evoke neuronal SICs. The poor specificity of the available pharmacological tools for studying the different purinergic receptors hampers, however, a clear identification of the distinct P2XR type that mediates SICs.

The tonic current, which was always associated with a noise increase in the current trace, was found to be mediated by a purinergic receptor different from the receptor that mediated SICs. The following observations suggest that the P2X$_7$R is a plausible candidate. (i) In contrast to SICs, the tonic current was sensitive to both BBG and OxATP; (ii) α,β-mATP, which in contrast to BzATP weakly activated P2X$_7$Rs (25, 37, 38), evoked SICs but failed to trigger the tonic current; (iii) the amplitude of BzATP-induced tonic current was greatly amplified in low extracellular Ca^{2+}, a condition that enhances P2X$_7$R openings (17, 37); (iv) the large amplitude tonic current evoked by BzATP in low extracellular Ca^{2+} was almost completely abolished in slices incubated with BBG; (v) in low Ca^{2+}, the weak P2X$_7$R agonist α,β-mATP triggered a tonic current of negligible amplitude compared with that triggered by BzATP under the same experimental conditions.

It is worth underlying that lowering extracellular Ca^{2+} results in a

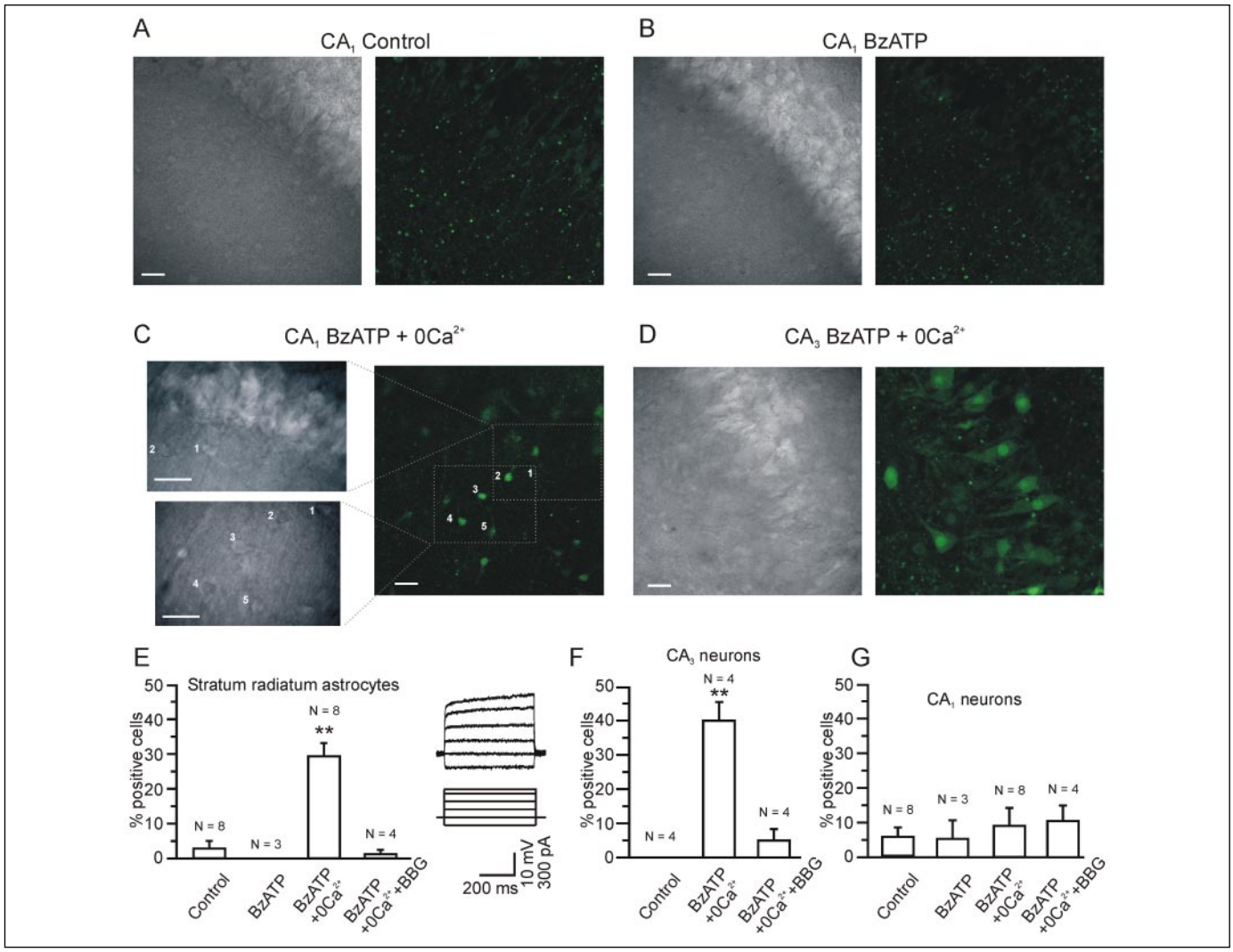

FIGURE 9. **Stratum radiatum astrocytes and CA3 neurons are permeabilized by BzATP stimulation with low extracellular Ca^{2+}.** *A–C*, differential interference contrast and corresponding fluorescence images of CA1 region under control conditions (*A*), in the presence of BzATP (*B*), and in the presence of BzATP and low Ca^{2+} (*C*). Images are the averages of 20 consecutive acquisitions. *Bar*, 20 μm. *D*, differential interference contrast and corresponding fluorescence images of CA3 region in the presence of BzATP and low Ca^{2+}. *Bar*, 20 μm. *E–G*, average percentage of positive stratum radiatum astrocytes (*E*, see the *inset* for passive membrane potential changes induced by current injections in whole-cell recording from a dye-loaded cell; $V_m = -61$ mV), CA3 (*F*), and CA1 (*G*) neurons under the different experimental conditions. The *numbers close* to the *bars* are the number of performed experiments. *, $p < 0.05$; **, $p < 0.01$.

2–3-fold increase in the amplitude of the NMDA receptor-mediated current and reduces inactivation of this receptor (39, 40). Although this change in NMDA receptor intrinsic properties may contribute to increase the amplitude of the tonic current triggered by BzATP-induced release of glutamate in low Ca^{2+}, it is highly unlikely that it can fully account for the observed 25-fold increase in the tonic current amplitude.

Besides enhancing the opening of P2X$_7$ receptors, lowering extracellular Ca^{2+} may also enhance hemichannel openings. Under these conditions, cytoplasmic glutamates of astrocytes have been reported to exit through these large conductance channels along its concentration gradient (41). Our results suggest that this release pathway does not contribute significantly to the tonic current, and the increase in background noise triggered by 100 μM BzATP in low Ca^{2+} since these events were not affected in the presence of the hemichannel blocker carbenoxolone. A reverse operation of the glutamate transporter is also unlikely to be involved since the tonic current and the increase in background noise were unchanged when BzATP was applied in the presence of TBOA, a potent inhibitor of glutamate transporters (31).

As to the cells that express the P2X$_7$R, astrocytes are good candidates. By reverse transcription-PCR analysis and Western blotting, astrocytes in culture have been shown to express, besides various P2YRs, all the P2XRs except the P2X$_6$R (34). Immunocytochemical studies in rat brain slices also revealed various P2XRs, including the P2X$_7$R, to be expressed in hippocampal astrocytes (42). In murine cultured astrocytes, BzATP has been reported to trigger a massive, slow efflux of glutamate into the extracellular space, suggesting that these cultured cells express functional P2X$_7$Rs (16). The following results from the present study are compatible with a functional expression of P2X$_7$Rs in hippocampal astrocytes *in situ*. (i) In all astrocytes recorded, in either voltage or current clamp configuration, a large amplitude inward current and a depolarization, respectively, slowly developed upon BzATP application; (ii) both responses were amplified in low Ca^{2+}, and they were almost completely blocked in slices incubated with BBG; (iii) in the presence of specific antagonists of AMPA, NMDA, and type I metabotropic glutamate receptors, BzATP-induced current was unchanged. Therefore, activation of these glutamate receptors in astrocytes by BzATP-induced release of glutamate does not contribute significantly to the BzATP-

induced current. These data also argue against the possibility that an increase in the extracellular concentration of K^+, which may derive from depolarizing neurons after activation by astrocytic glutamate of AMPA and NMDARs, is involved in BzATP-induced currents in astrocytes; (iv) in a fluorescent dye permeability assay, a BBG-sensitive uptake of lucifer yellow was detected in astrocytes upon stimulation with BzATP in low Ca^{2+}. Dye loading was undetectable in slices incubated with normal Ca^{2+} as well as in slices incubated with normal Ca^{2+} and BzATP.

According to these observations, BzATP application should open in the astrocytic membrane a non-selective channel, such as a P2X$_7$R that in the large pore configuration allows cations such as K^+, Na^+, and Ca^{2+} and anions such as Cl^- and glutamate to flow through the membrane according to their electrochemical gradient, ultimately driving the reversal potential of the whole-cell I-V relationship to more positive values. During BzATP application, the I-V curve was indeed observed to shift significantly along the voltage axis in the depolarizing direction. Although this result is compatible with the opening of a P2X$_7$-like receptor, the overall membrane conductance was surprisingly found to be unchanged upon BzATP application and to decrease drastically after BzATP washout. A possible interpretation of this contradictory result is that the expected increase in membrane conductance due to P2X$_7$-like receptor openings is masked by the overall decrease in membrane conductance that is triggered by BzATP and becomes evident only after BzATP washout.

Taken together, results obtained are compatible with the view that P2X$_7$R openings in astrocytes lead to formation of a large conducting pore that allows the uptake of molecules of relatively large molecular weight. Further experiments are necessary to provide conclusive evidence on this issue.

BzATP applied in normal Ca^{2+} evoked a tonic current response in 35% of neurons, whereas it evoked an inward current in all astrocytes tested. A plausible hypothesis for this discrepancy is that the variability of the neuronal response reflects the non uniform organization of astrocyte-neuron contacts in the hippocampus (43). Neurons unresponsive to BzATP may be located far away from astrocyte processes and display a tonic current only when the release of glutamate from astrocytes is greatly potentiated, as in the case of BzATP applied in low Ca^{2+}. Indeed, when BzATP was applied in low Ca^{2+}, the tonic current response was observed in all neurons. Noteworthy is that the same neurons that did not display a detectable response to a first BzATP challenge in normal Ca^{2+} displayed a clear tonic current in response when a second BzATP challenge was applied in low Ca^{2+}.

In the hippocampus, besides astrocytes, CA3 pyramidal neurons as well as neurons from the dentate gyrus have been reported to express the P2X$_7$R (44–46). Although this point was not addressed in detail here, we observed that in slices incubated with low Ca^{2+} and BzATP, a BBG-sensitive uptake of the dye was detected in a subpopulation of CA3 neurons. Glutamate released through P2X$_7$Rs expressed on CA3 axon terminals of Schaffer collateral pathway may, thus, contribute to the tonic current that we recorded from CA1 neurons.

As to the functional role that glutamate derived from P2X$_7$R activation may have, it has to be taken into account that the endogenous agonist of purinergic receptors, ATP, is a weak P2X$_7$R agonist. It is, thus, unlikely that ATP released under physiological conditions from either axon terminals of Schaffer collaterals (47) and/or astrocytes (35, 48) can reach the high extracellular concentration that is necessary to activate the P2X$_7$R. Most importantly however, such a high concentration may be reached under pathological conditions, such as ischemia and brain trauma (49). The consequent activation of P2X$_7$Rs may result in a massive glutamate release and contributes to increase the extracellular glutamate to the abnormal levels that cause excitotoxic cell death (50). Consistent with this hypothesis, P2X$_7$R inhibition has been recently found to improve the functional recovery and to decrease the death of motoneurons after acute spinal cord injury in rats (51).

It has to be underlined that the expression of the P2X$_7$R in brain cells other than activated microglia (17, 18) is highly debated (52), and conflicting results have been reported. Although previous studies provide indications for the presence of the P2X$_7$R in both astrocytes (42) and neurons from the CA1, CA3, and dentate gyrus region (44, 45, 53, 54), more recent studies cast serious doubts on this conclusion (55, 56).

The results reported in the present study are compatible with the functional expression of the P2X$_7$R in hippocampal cells, either astrocytes and/or neurons. However, also due to the lack of highly specific agonists and antagonists for the different purinergic receptors, we can only suggest that the release of glutamate which triggers the tonic current is due to the activation of the P2X$_7$R- or a P2X$_7$-like receptor. Indeed, other P2XRs, such as the P2X$_2$R and the P2X$_4$R, that have been suggested to result in a progressive formation of a large conducting pore (57, 58) are expressed in stratum radiatum astrocytes (42) and may, thus, be involved in the generation of the tonic current.

In conclusion, the results here reported clearly demonstrate that activation of different purinergic receptors in the hippocampus mediates two types of glutamate release, each evoking a distinct response in CA1 pyramidal neurons. In the first type of release, the P2X$_7$R is not involved. This type of glutamate release from astrocytes evokes in CA1 pyramidal neurons transient NMDAR-mediated responses (SICs) that represent a hallmark of astrocyte-to-neuron communication (11). In the second type of release, the P2X$_7$R or a P2X$_7$-like receptor, may be involved. This release triggers a slowly developing, tonic current and contributes to increase the concentration of extracellular glutamate. This event is potentiated under non-physiological conditions, raising the possibility that it contributes to the excitotoxic action of glutamate in the brain.

Acknowledgments—We thank P. G. Haydon and F. Di Virgilio for critical reading of the manuscript.

REFERENCES

1. Choi, D. W. (1988) *Neuron* **1,** 623–634
2. Choi, E. S. H., and Clegg, D. O. (1990) *Dev. Biol.* **142,** 169–177
3. Parpura, V., Basarsky, T. A., Liu, F., Jeftinija, K., Jeftinija, S., and Haydon, P. G. (1994) *Nature* **369,** 744–747
4. Pasti, L., Volterra, A., Pozzan, T., and Carmignoto, G. (1997) *J. Neurosci.* **17,** 7817–7830
5. Bezzi, P., Carmignoto, G., Pasti, L., Vesce, S., Rossi, D., Rizzini, B. L., Pozzan, T., and Volterra, A. (1998) *Nature* **391,** 281–285
6. Newman, E. A., and Zahs, K. R. (1998) *J. Neurosci.* **18,** 4022–4028
7. Kang, J., Jiang, L., Goldman, S. A., and Nedergaard, M. (1998) *Nat. Neurosci.* **1,** 683–692
8. Liu, Q.-S., Xu, Q., Arcuino, G., Kang, J., and Nedergaard, M. (2004) *Proc. Natl. Acad. Sci. U. S. A.* **101,** 3172–3177
9. Fiacco, T. A., and McCarthy, K. D. (2004) *J. Neurosci.* **24,** 722–732
10. Angulo, M. C., Kozlov, A. S., Charpak, S., and Audinat, E. (2004) *J. Neurosci.* **24,** 6920–6927
11. Fellin, T., Pascual, O., Gobbo, S., Pozzan, T., Haydon, P. G., and Carmignoto, G. (2004) *Neuron* **43,** 729–743
12. Kreft, M., Stenovec, M., Rupnik, M., Grilc, S., Kržan, M., Potokar, M., Pangršic, T., Haydon, P. G., and Zorec, R. (2004) *Glia* **46,** 437–445
13. Bezzi, P., Gundersen, V., Galbete, J. L., Seifert, G., Steinhäuser, C., Pilati, E., and Volterra, A. (2004) *Nat. Neurosci.* **7,** 613–620
14. Evanko, D. S., Zhang, Q., Zorec, R., and Haydon, P. G. (2004) *Glia* **47,** 233–240
15. Fellin, T., and Carmignoto, G. (2004) *J. Physiol.* (*Lond.*) **559,** 3–15
16. Duan, S., Anderson, C. M., Keung, E. C., Chen, Y., and Swanson, R. A. (2003) *J. Neurosci.* **23,** 1320–1328
17. Di Virgilio, F. (1995) *Immunol. Today* **16,** 524–528

18. Di Virgilio, F., Chiozzi, P., Ferrari, D., Falzoni, S., Sanz, J. M., Morelli, A., Torboli, M., Bolognesi, G., and Baricordi, O. R. (2001) *Blood* **97,** 587–600
19. Jeremic, A., Jeftinija, K., Stevanovic, J., Glavaski, A., and Jeftinija, S. (2001) *J. Neurochem.* **77,** 664–675
20. Coco, S., Calegari, F., Pravettoni, E., Pozzi, D., Taverna, E., Rosa, P., Matteoli, M., and Verderio, C. (2003) *J. Biol. Chem.* **278,** 1354–1362
21. Edwards, F. A., Konnerth, A., Sakmann, B., and Takahashi, T. (1989) *Pfluegers Arch. Eur. J. Physiol.* **414,** 600–612
22. Matthias, K., Kirchhoff, F., Seifert, G., Hüttmann, K., Matyash, M., Kettenmann, H., and Steinhäuser, C. (2003) *J. Neurosci.* **23,** 1750–1758
23. Mulligan, S. J., and MacVicar, B. A. (2004) *Nature* **431,** 195–199
24. North, R. A., and Surprenant, A. (2000) *Annu. Rev. Pharmacol. Toxicol.* **40,** 563–580
25. Lambrecht, G. (2000) *Naunyn-Schmiedebergs Arch. Pharmacol.* **362,** 340–350
26. Jiang, L.-H., Mackenzie, A. B., North, R. A., and Surprenant, A. (2000) *Mol. Pharmacol.* **58,** 82–88
27. Murgia, M., Hanau, S., Pizzo, P., Rippa, M., and Di Virgilio, F. (1993) *J. Biol. Chem.* **268,** 8199–8203
28. Gerber, U., Greene, R. W., Haas, H. L., and Stevens, D. R. (1989) *J. Physiol.* (*Lond.*) **417,** 567–578
29. North, R. A. (2002) *Physiol. Rev.* **82,** 1013–1067
30. Burgo, A., Carmignoto, G., Pizzo, P., Pozzan, T., and Fasolato, C. (2003) *J. Physiol.* (*Lond.*) **549,** 537–552
31. Shimamoto, K., Lebrun, B., Yasuda-Kamatani, Y., Sakaitani, M., Shigeri, Y., Yumoto, N., and Nakajima, T. (1998) *Mol. Pharmacol.* **53,** 195–201
32. Kamermans, M., Fahrenfort, I., Schultz, K., Janssen-Bienhold, U., Sjoerdsma, T., and Weiler, R. (2001) *Science* **292,** 1178–1180
33. Peters, O., Schipke, C. G., Hashimoto, Y., and Kettenmann, H. (2003) *J. Neurosci.* **23,** 9888–9896
34. Fumagalli, M., Brambilla, R., D'Ambrosi, N., Volonte, C., Matteoli, M., Verderio, C., and Abbracchio, M. P. (2003) *Glia* **43,** 218–230
35. Bowser, D. N., and Khakh, B. S. (2004) *J. Neurosci.* **24,** 8606–8620
36. Bianchi, B. R., Lynch, K. J., Touma, E., Niforatos, W., Burgard, E. C., Alexander, K. M., Park, H. S., Yu, H., Metzger, R., Kowaluk, E., Jarvis, M. F., and van Biesen, T. (1999) *Eur. J. Pharmacol.* **376,** 127–138
37. Ralevic, V., and Burnstock, G. (1998) *Pharmacol. Rev.* **50,** 413–492
38. North, R. A., and Barnard, E. A. (1997) *Curr. Opin. Neurobiol.* **7,** 346–357
39. Gorter, J. A., and Brady, R. J. (1995) *Neurosci. Lett.* **194,** 209–213
40. Chen, N., Murphy, T. H., and Raymond, L. A. (2000) *J. Neurophysiol.* **84,** 693–697
41. Ye, Z.-C., Wyeth, M. S., Baltan-Tekkok, S., and Ransom, B. R. (2003) *J. Neurosci.* **23,** 3588–3596
42. Kukley, M., Barden, J. A., Steinhäuser, C., and Jabs, R. (2001) *Glia* **36,** 11–21
43. Ventura, R., and Harris, K. M. (1999) *J. Neurosci.* **19,** 6897–6906
44. Atkinson, L., Batten, T. F., Moores, T. S., Varoqui, H., Erickson, J. D., and Deuchars, J. (2004) *Neuroscience* **123,** 761–768
45. Cavaliere, F., Amadio, S., Sancesario, G., Bernardi, G., and Volonté, C. (2004) *J. Cereb. Blood Flow Metab.* **24,** 392–398
46. Deuchars, S. A., Atkinson, L., Brooke, R. E., Musa, H., Milligan, C. J., Batten, T. F. C., Buckley, N. J., Parson, S. H., and Deuchars, J. (2001) *J. Neurosci.* **21,** 7143–7152
47. Pankratov, Y., Castro, E., Miras-Portugal, M. T., and Krishtal, O. (1998) *Eur. J. Neurosci.* **10,** 3898–3902
48. Zhang, J.-m., Wang, H.-k., Ye, C.-q., Ge, W., Chen, Y., Jiang, Z.-l., Wu, C.-p., Poo, M.-m., and Duan, S. (2003) *Neuron* **40,** 971–982
49. Fields, R. D., and Stevens, B. (2000) *Trends Neurosci.* **23,** 625–633
50. Choi, D. W., and Rothman, S. M. (1990) *Annu. Rev. Neurosci.* **13,** 171–182
51. Wang, X., Arcuino, G., Takano, T., Lin, J., Peng, W. G., Wan, P., Li, P., Xu, Q., Liu, Q. S., Goldman, S. A., and Nedergaard, M. (2004) *Nat. Med.* **10,** 821–827
52. Khakh, B. S. (2001) *Nat. Rev. Neurosci.* **2,** 165–174
53. Armstrong, J. N., Brust, T. B., Lewis, R. G., and MacVicar, B. A. (2002) *J. Neurosci.* **22,** 5938–5945
54. Sperlágh, B., Köfalvi, A., Deuchars, J., Atkinson, L., Milligan, C. J., Buckley, N. J., and Vizi, E. S. (2002) *J. Neurochem.* **81,** 1196–1211
55. Sim, J. A., Young, M. T., Sung, H.-Y., North, R. A., and Surprenant, A. (2004) *J. Neurosci.* **24,** 6307–6314
56. Kukley, M., Stausberg, P., Adelmann, G., Chessell, I. P., and Dietrich, D. (2004) *J. Neurosci.* **24,** 7128–7139
57. Khakh, B. S., Bao, X. R., Labarca, C., and Lester, H. A. (1999) *Nat. Neurosci.* **2,** 322–330
58. Virginio, C., MacKenzie, A., Rassendren, F. A., North, R. A., and Surprenant, A. (1999) *Nat. Neurosci.* **2,** 315–321

Purinergic Receptors Mediate Two Distinct Glutamate Release Pathways in Hippocampal Astrocytes

Tommaso Fellin, Tullio Pozzan and Giorgio Carmignoto

J. Biol. Chem. 2006, 281:4274-4284.
doi: 10.1074/jbc.M510679200 originally published online December 6, 2005
